OXIDATION OF TBC COATED NICKEL BASED SUPERALLOYS AND GAMMA TITANIUM ALUMINIDES FOR LAND-BASED ENGINES

–

BY

DENNIS AMOA-ASIAMAH

A THESIS

SUBMITTED TO THE AFRICAN UNIVERSITY OF SCIENCE AND TECHNOLOGY

ABUJA – NIGERIA

IN PARTIAL FULFILLMENT OF THE REQUIREMENTS FOR THE

AWARD OF MASTER OF SCIENCE IN (MATERIALS SCIENCE AND ENGINEERING)

SUPERVISOR: PROF. WINSTON OLUWOLE SOBOYEJO

Abstract

Our ability to power modern airplanes and land based engines depends largely on the thrust generated most importantly by aero engines. Over the past 30 years material cost has become an important factor, especially in commercial aero engines where light weight and high temperature materials are needed for improved efficiency and specific thrust. The required combinations of high temperature properties has led to the applications of nickel-based superalloys and most recently gamma based titanium aluminides in gas sections of aeroengine. This thesis examines the high temperature oxidation behavior of nickel based alloys and gamma titanium aluminides with thermal barrier coatings. The kinetics of oxidation of the coated structures has been studied at various temperatures (800, 900, 1000^0C) that are relevant to gas turbine engines. In this study, the effects of oxidation on the stress intensity factor (mode I and mode II cracks) and the energy release rate are computationally simulated using the ABAQUS^{TM} software. Results are discussed in relation to the principal strain in the top coat/TGO interface. The implications of the results are discussed for the design of improved land-based engines and aero-engines.

Acknowledgement

I thank God for His Mercies and Grace and also for giving me the privilege to pursue a master's degree in this noble institution. With God on my side I was able to achieve academic excellence throughout my stay on the African University of Science and technology campus.

Secondly, my gratitude goes to my supervisor Professor Winston Oluwole Soboyejo for his fatherly direction and tremendous input in this thesis. But for your supervision Prof, I wouldn't have gotten this far.

Thirdly, my endless appreciation goes to my co-supervisor, Dr. Patrick Mensah of Southern University for his extraordinary support and the African Development Bank (AfDB) for the scholarship package.

Finally, I would like to acknowledge all the PhD students especially Chukwuemeka Joseph Ani and all the MSc. Students of African University of Science and technology.

Dedication

I dedicate this thesis to lord Almighty, the entire staff of the North and South heap leach, my family and most especially my dear friend Alexander Ofori Asomani.

Table of Contents

List of Figures

Chapter One

1.0 Background and Introduction

1.1 Background

The need for high temperature engines for land-based and aero applications has resulted in massive research in the last 30 years [1-5]. It is relevant for these engines to have high temperatures in order to get better performance and better efficiency [6]. The incremental way to attain these high temperatures (1100^0C-1150^0C) without causing damage to the material is the use of a thermal barrier coating (TBC) [2] or an environmental barrier coating (EBC) [7].Nevertheless, these coating systems begin to spall due to a range of mechanisms that include oxidation and creep [8].Although nickel base superalloys have been used at high temperatures, they have shown substantial resistances to time depend creep [5]. However, the density limits it's in application where weight is a major concern. It is therefore important to better understand the afore-mentioned mechanisms in order to slow them down and improve the service performance of these materials. Titanium Aluminide (Ti-48Al-2Cr-2Nb) is an intermetallic compound which is being considered in this application because of its reduced density as well as its high temperature capability [9]. Nonetheless, developing mechanism-based model for the prediction of high temperature oxidation and creep will make quiet a contribution in this field.

1.2 Introduction

Nickel-based superalloys are a group of metallic materials which contain more than six alloying elements (Mo, W, Nb, Al, C and Cr) and nickel as a base element [1].The type of alloying depends on the level of development of nickel-based superalloys in the aeroengine manufacturing industry. For this reason, several generations of nickel-based superalloys have been produced [3]. In recent times nickel-based superalloys have been alloyed with heavy elements such as rhenium and ruthenium [3] to prevent diffusion and grain boundary rotation. These elements also prevent the diffusion which is associated with creep [10]. Other element like chromium has been added to the superalloy to control/prevent corrosion [3]. As technology progresses in the aero-industry, more alloying elements will be added to nickel-based superalloys to get the desired properties in that regard.

Another challenge that has been of major concern to the aero-industry is weight [5]. This is because nickel-based superalloys constitute 40-50% of the entire weight of the aeroengine [11]. The weight of an aircraft/land-based engine affects the thrust [13] and fuel consumption [5]. Aircraft/land based engines manufacturers have allocated funds in research to engineer new robust lightweight materials and can be used in aero-engines. Pratt and Whitney [12] have researched into the use of titanium metal matrix composites and gamma titanium aluminides (Ti-48Al-2Cr-2Nb) as possible substitutes of nickel-based superalloys. Gamma titanium aluminide have a density ($4.2g/cm^3$) which is approximately half the density of nickel ($8.4g/cm^3$) [13]. The successful use of gamma titanium aluminide (Ti-48Al-2Cr-2Nb) in some sections of the aero engine tends to

reduce the overall weight [5], improve the thrust[13] and efficiency[13] and reduce the fuel consumption of the engine [5].

Although gamma titanium aluminide is being considered, its mechanical properties may not be the same as nickel-based superalloys. However, its overall mechanical property to weight ratio makes the intermetallic more attractive than nickel-based superalloys [13]. Research has shown that the intermetallic ductility can be improved by alloying with elements such as chromium [14]. However, there are other challenges associated with the intermetallic. Below 800^0C the alloy has been shown to form four layers (TiO_2 ,Al_2O_3 and TiO_2 , Al_2O_3 and TiAl). The formation of TiO_2 results in problems such as oxidation but since the alumina content in the layer is more than the TiO_2, it tends to suppress its effects on the substrate. Furthermore, above 800^0C there is a reduction in oxidation resistance because of the formation of more TiO_2 than Alumina [13] which is a non-protective oxide. Thermal Barrier Coating (TBC) is a coating system that has been used to reduce the possible occurrence of oxidation at 800^0C. This is because TBCs has the ability to achieve a temperature differential experienced by the gamma titanium aluminide (Ti-48Al-2Cr-2Nb) substrate by 175^0C [8].

Most recently, interfacial delamination [15] and other failure processes associated with diffusion [16] have raised a lot of concerns. A TBC system consists of three distinct layers. This layers are the top coat (TC), the thermally grown oxide layer (TGO) and the bond coat (BC) [8]. Various techniques have been used to deposit TBC on substrates. These techniques are Electron Beam Physical Vapor Deposition (EB-PVD) [17], Air plasma Spraying [14] and High Velocity Oxygen Fuel (HVOF) [18]. The deposition methods can help reduce the occurrence of some of these challenges. A lot of [2, 3, 8,

15, 16, 17] research has been done from this direction. Soboyejo et al in 2010 compared the oxidation of vertically cracked sample to the conventional TBC system. They concluded that the vertically cracked sample gave a better oxidation resistance [17]. Also, Saremi et al., 2007 investigated the oxidation resistance of a TBC system. They coated the bond coat with alumina and compared its oxidation resistance with a conventional TBC system. The authors found that Alumina-coated bond coat thermal barrier coating have a good oxidation resistance [16].Essentially, engineering a better deposition system or introducing cracks or any form of defect in carefully controlled manner may have significant influence on a TBC system.

This work explores the development of mechanism-based models for the prediction of the combined effects of high temperature oxidation and creep. First, the stresses due to the oxidation behavior of the layers in a thermal barrier coating were determined by experiments. The induced creep due to the stresses associated with the oxidation of the thermally grown oxide (TGO) layer was modeled along with the crack driving forces associated with crack growth and film spallation. The implications of the results were discussed for the design of robust TBCs and the development of mechanism –based life prediction approaches.

1.3 Objectives

The objective of this research is to:

- Develop a mechanism based approach to fundamentally understand the oxidation in thermal barrier coating systems and investigate the driving force of crack growth in the TBC system.
- To determine the effects of TGO growth on energy release rate.
- To finally improve the efficiency of land based engines using TBC coated gamma titanium aluminide and the results from the above.

1.4 Scope of work

Chapter one gives a background and introduces the thesis work. In this chapter, general or first-hand information of what the thesis work is all about is unfolded. A scientific problem is well posed, unresolved issues are identified, and objectives of the thesis spelt out clearly and the approach to solving the problem are clearly outlined.

Chapter two gives in-depth observations that have been made through reviewing literature. In this chapter nickel based superalloy, gamma titanium aluminide and thermal barrier coatings (TBCs) are introduced. The aforementioned alloying elements, microstructure and application are described. Prior works that have been done in this field of study have also been thoroughly investigated in this chapter.

Chapter three presents the experimental processes carried out. The materials and methods used in the experiment are also listed. The steps or procedure that was followed in the fabrication of a thermal barrier coating is outlined. Sample preparation and some

characterization techniques used on the samples are present in this chapter. Finally, the oxidation temperature and times is stated in this chapter for the experiment.

Chapter four discusses the modeling and simulation that have been carried out to verify the experimental results.

Chapter five describes the outcome or results of both experiment and modeling. Also, the implications of the results are thoroughly discussed in this chapter.

Chapter six concludes the thesis work; that is the experiments, modeling, results and implication is summarized. The future work however is considered and some recommendations are made in this chapter.

References:

[1] Jovanović, M. T., et al. "Processing and Some Applications Of Nickel, Cobalt and Titanium-Based Alloys" AMES.

[2] J.T. DeMasi-Marcin and D.K. Gupta, “Protective coatings in the gas turbine engine” Surface and Coatings Technology, 68/69 (1994), pp.1-9.

[3] Tresa M. Pollock and Sammy Tin, Nickel-Based Superalloys for Advanced Turbine Engines: Chemistry, Microstructure, and Properties, Journal of Propulsion and Power Vol. 22, No. 2, March–April 2006.

[4] Alain Lasalmonie Intermetallics: Why is it so difficult to introduce them in gas turbine engines? Intermetallics 14 (2006) 1123-1129.

[5] Singh, Antariksh Rao Pratap. Mechanisms of ordered gamma prime precipitation in

nickel base superalloys. PhD thesis, 2011.

[6] Bose S., J. DeMasi-Marcin, “Thermal Barrier Coating Experience In Gas Turbine Engines At Pratt And Whitney”, Thermal Barrier Coating Workshop, NASA CP 3312, 1995, p. 63.

[7] E. K. Arthur, E. Ampaw, S. T. Azeko, Y. Danyuo, B. Agyei-Tuffour, K. Kan-Dapaah, J. D. Obayemi Design of Thermally Reliable Environmental Barrier Coating for a SiC/SiC Ceramic Matrix Composites. International Journal of Composite Materials 2013, 3(6): 191-197.

[8] N.M. Yanar, M.J. Stiger, et al., “The effects of high temperature exposure on the Durability of Thermal Barrier Coatings”, Key Engineering Materials Vol. 197, pp. 145-164, 2001.

[9] Bartolotta, P, et al., **“**The Use of Cast Ti-48Al-2Cr-2Nb in Jet Engines”, *Journal of Material (JOM).* 1997, pp. 48-50, 76.

[10] VerSnyder, F. L., and Shank, M. E., “Development of Columnar Grain and Single Crystal High-Temperature Materials Through Directional Solidification,” *Materials Science and Engineering*, Vol. 6, No. 4, 1970, pp. 213–247.

[11] Schafrik, R., and Sprague, R., “Saga of Gas Turbine Materials: Part III,”Advanced Materials and Processes, Vol. 162, May 2004, pp. 27–30.

[12] Singerman, S. A., et al. "Titanium metal matrix composites for aerospace applications." *Superalloys 1996, Proceedings of Eighth International Symposium on Superalloys*. TMS, Warrendale, PA, 1996.

[13] Sanna Fager Franzén, “γ-Titanium Aluminide Manufactured by Electron Beam Melting” ,thesis ,2010.

[14] Westbrock, Jack Hall and Fleischer, Robert Louis**,** Intermetallic Compounds Principles and Practice - Volume 2 Practice. West Sussex : John Wiley & Sons Ltd, 1995.

[15] Deng, H.X.. "Effect of heat treatment at 900^oC on microstructural and mechanical properties of thermal barrier coatings", Surface & Coatings Technology, 2011/03/15

[16] Saremi, M., "Microstructural analysis of YSZ and YSZ/Al_2O_3 plasma sprayed thermal barrier coatings after high temperature oxidation", Surface & Coatings Technology, 2008/04/15.

[17] W.O. Soboyejo,P.Mensah, R. Diwan, J. Crowe and S. Akwaboa, High Temperature Oxidation Interfacial Growth Kinetics in YSZ Thermal barrier Coatings with Bond Coatings of NiCoCrAlY with 0.25% Hf, Materials Science and Engineering A, Vol. 528, page 2223-2230, 2011.

[18] D. Cheng, G. Trapaga., et al. Mathematical Modelling of High Velocity Oxygen Fuel thermal Spraying: An Overview, Key Engineering Materials Vol. 197(2001) pp.1-26.

Chapter two

Literature Survey

2.0 Introduction

Superalloys can be said to be known as high temperature alloy [1]. This is because these alloys tend to exhibit exceptional mechanical properties at high temperatures [2]. Other important characteristics have made superalloys center of attraction in the last 30 years [3].However, above 850^0C nickel based superalloys tend to loss their corrosion resistance properties [4]. High melting points elements such as nickel, cobalt or nickel-iron in balanced compositions in an alloy is the bases on which an alloy can be classified as a superalloy. Aerospace, power generation industries and chemical processing plants have been dependent on the use of superalloys due to their process conditions and temperatures [5]. Over the past few years development of next generation superalloys have been centered on these industries. Advances have been made in superalloy development in terms of their high strength at high temperature by solid solution strengthening [6]. Most significantly, precipitation strengthening is encouraged when a second phase gamma prime and carbide precipitate is produced. Thermal Barrier Coatings (TBCs) or Thermal Protective Systems (TPS) are used to tackle the adverse effect of oxidation and corrosion in superalloys. Intrinsic problems such as oxidation and corrosion are tackled by using chromium and aluminum [7].

Mode of Operation of An Aeroengine

The thrust generated by aeroengines have been of major concern for manufacturers. Due to this challenge, some manufacturers have resorted to using extra aeroengines to help curb this issue. A lot of research has gone into the use of composite materials for modern airplanes. Material cost and some processing techniques have however been of major "headache" to manufacturers. Some of these challenges can be understood if and only if engine designers and manufacturers will resort to the mode of operation of the aeroengine.

A modern aeroengine consist of three main sections. These sections in order of increasing temperatures experienced are the fan, compressor and turbine. It is important to note that in each of these sections, low and high pressures are experienced. The fan which may be made from titanium alloy or PMC accepts air which passes through the multiple stages of the compressor. The compressor which is principally composed of disks and blades are also manufactured from titanium alloys (Ti-6Al-4V). Relatively low temperatures are experienced in the fan and aeroengine sections of the aeroengine [8]. Temperatures of about 400-500^{0}C may be recorded in the high pressure stages. In the combustor section, the air is ignited and expanded through the different stages of the turbine and the nozzle which is fabricated from niobium at the end of the engine. Due to high temperatures (500-650^{0}C) experienced in the combustor and turbine sections (especially in the disks), nickel and cobalt based superalloys are used. The tip of the blade sees a much high temperature (1200^{0}C). The microstructure and constituent of the superalloys are also engineered to produce the needed blend of creep, strength, fatigue and oxidation

resistance needed for performance in aeroengine that rotate at an angular speed of 20,000rev/minute [8].

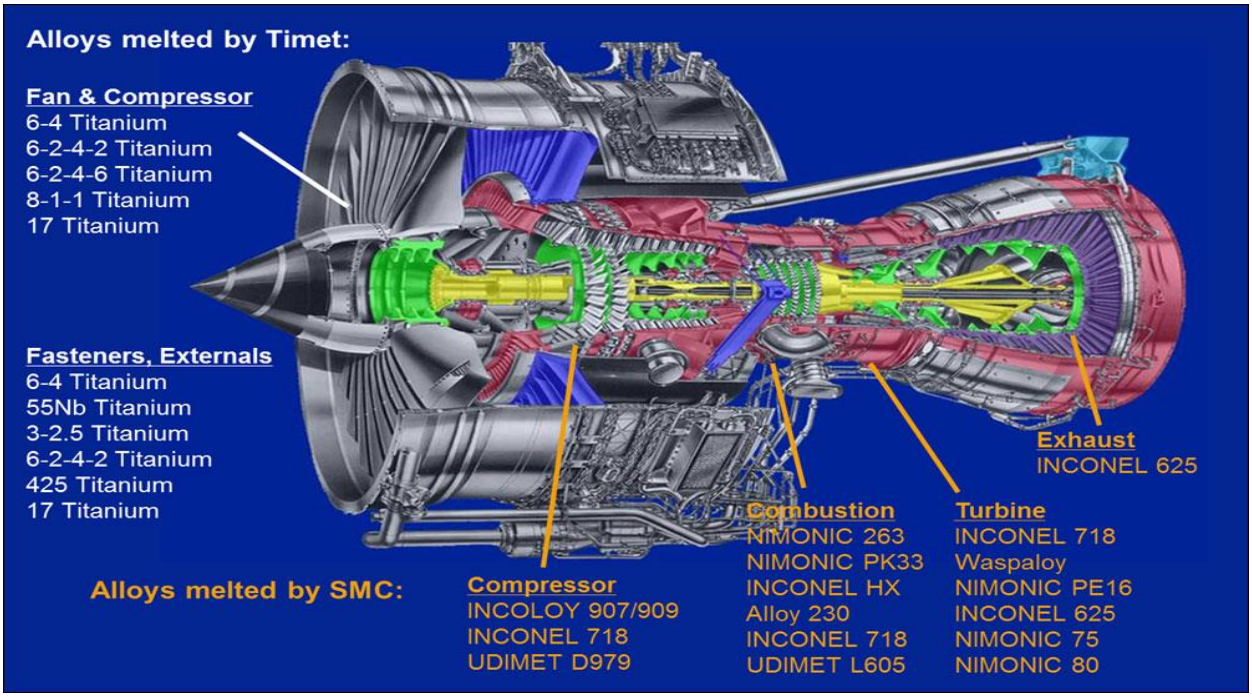

Figure 2. 1: *Nickel alloys used in the various parts of the aeroengine adapted from pccforgedproducts.com*

2.1 Nickel based Superalloys

Nickel-based superalloys over the past 30 years are used in numerous applications [9]. The most eminent use is in the fabrication of gas turbines for commercial and military aircraft, power generation, and marine propulsion. The superalloy, due to its attractive properties also finds its use in space vehicles, the oil and gas industry, nuclear reactors, military electric motors, heat exchanger tubing, chemical processing vessels, and submarines [9]. Batches of super alloys have been produced, due to the need of balanced properties and each generation seems to have higher temperature resistance as research proceeds. Highly expensive heavy alloying elements such as rhenium and ruthenium have been used in the latest batch of superalloys to achieve the desired properties. As a result, cost have been of major concern since some new generation of superalloys can be five times more expensive than high-quality turbine steel[9]. As the aircraft manufacturing and electrical power generation industries grow, the effect of cost will be greatly felt especially in countries where these elements are not being mined.

Although nickel based superalloys have exceptional high temperature properties (high fracture toughness, resistance to degradation in oxidizing environment and high temperature strength), the density however result in the alloy constituting approximately 40-50% of the entire weight of an aeroengine [10-15]. Processing techniques has however, reduced the occurrence of creep. This can further be explained by the use of complex investment casting technique to produce turbine blades and vanes with controlled grain size [15]. Consequently, such casting procedure is likely to produce columnar or equiaxed grain or a single crystal so as to get rid of high angle grain boundaries [15,16]. Eliminating high angle grain boundaries is very significant since they

are site for failure which normally occurs as a result of reactiveness [16]. Based on this reason single crystal blades [17] are preferred in the early stages of the gas turbine whereas equiaxed structures are preferred in the later (cooler) stages of the turbine. A stage is a set of blades and vanes arranged in a row.

A lower concentration(less than 10 atomic %) of aluminum and titanium are significant solutes in nickel based superalloys. This solutes results in the formation of a two phase equilibrium microstructure consisting of a mixture of gamma (γ) and gamma prime (γ'). Increasing the content of aluminum in gamma nickel results in the formation of a second precipitate phase [15]. Ni_3Al is the resulting ordered intermetallic second phase formed has an L12 crystal structure [15]. The elevated temperature strength and creep resistance is largely dependent on the gamma prime phase of a nickel based superalloy.

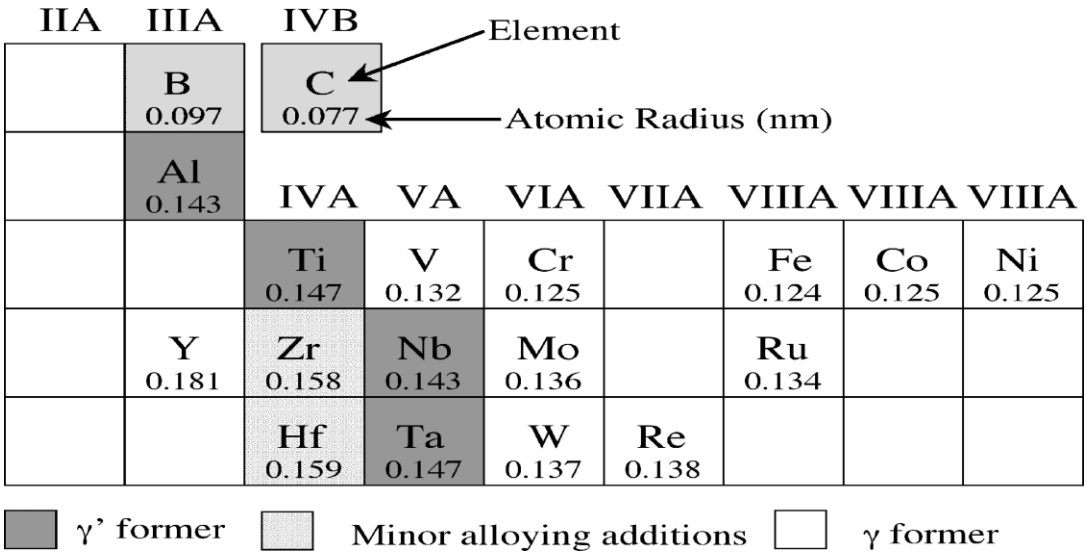

Figure 2. 2: *Alloying elements present in Ni-based superalloys (adapted from reference 15)*

When the supersaturated solid solution of γ nickel is cooled below its equilibrium solvus temperature, the γ' phase is formed and occurs in solid state. The cooling rate at this point is significant in the precipitation and growth kinetics of the γ phase. The cooling rate(in excess of ~40 K/min) is affected by the unimodal distribution of fine γ precipitate (300-500nm),therefore slow cooling rate results in multiple populace of γ' precipitates made up of the small (<50nm) and large (>500nm) precipitate sizes [15]. Increasing the number of alloying element does not result in the formation of any distinct phase other than the two principal phases (γ *and* γ') in the microstructure of the nickel based superalloy. Refractory alloying elements (Mo, W, Nb and Re) are added for solid solution strengthening of the γ phase whereas the γ' phase is strengthened by the addition of Ti, Ta and Nb [15].

Nickel based superalloys are typically alloyed with Chromium, cobalt, molybdenum, tungsten, tantalum, rhenium, niobium, aluminum, titanium, hafnium, carbon, boron, yttrium and zirconium [11]. The alloying levels depend on the applications and [15] processing route. The alloys also include: conventional cast alloys, directionally solidified alloys, first to third generation single crystal alloys, wrought superalloys and powder processed superalloys [15].

2.1.1 Applications of Nickel Based Superalloys

Nickel based superalloys find their application in different section of a turbine.

2.1.1.0 Turbine Blades

A major use of nickel based superalloys is in the manufacture of aeroengine turbine blades. A single-crystal blade is free from γ/γ grain boundaries. Boundaries are easy diffusion paths and therefore reduce the resistance of the material to creep deformation. The directionally solidified columnar grain structure has many γ grains, but the boundaries are mostly parallel to the major stress axis; the performance of such blades is not as good as the single-crystal blades. However, they are much better than the blade with the equiaxed grain structure which has the worst creep life. One big advantage of the single-crystal alloys over conventionally cast polycrystalline superalloys is that many of the grain boundary strengthening solutes are removed. This results in an increase in the incipient melting temperature (i.e., localized melting due to chemical segregation). The single-crystal alloys can therefore be heat treated to at temperatures in the range 1240-1330°C, allowing the dissolution of coarse γ' which is a remnant of the solidification process. Subsequent heat treatment can therefore be used to achieve a controlled and fine-scale precipitation of γ'. The primary reason why the first generation of single-crystal superalloys could be used at higher temperatures than the directionally solidified ones, was because of the ability to heat-treat the alloys at a higher temperature rather than any advantage due to the removal of grain boundaries. A higher heat-treatment temperature allows all the γ' to be taken into solution and then by aging, to precipitate in a finer form. Superalloys blades are used in aeroengines and gas turbines in regions where the temperature is in excess of about 400^{o}C, with titanium blades in the colder regions. This

is because there is a danger of titanium igniting in special circumstances if its temperature exceeds 400^{o}C.

2.1.1.1 Turbine Discs

Turbine blades are attached to a disc which in turn is connected to the turbine shaft. The properties required for an aeroengine discs are different from that of a turbine, because the metal experiences a lower temperature. The discs must resist fracture by fatigue. Discs are usually cast and then forged into shape. They are polycrystalline.

2.1.1.2 Superalloys Disc

One difficulty is that cast alloys have a large columnar grain structure and contain significant chemical segregation; the latter is not completely eliminated in the final product. This can lead to scatter in mechanical properties. One way to overcome this is to begin with fine, clean powder which is then consolidated. The powder is made by atomisation in an inert gas; the extent of chemical segregation cannot exceed the size of the powder. After atomisation, some discs are made from powder which is hot-isostatically pressed, extruded and then forged into the required shape. The process is difficult because of the need to avoid undesired particles introduced, for example, from the refractories used in the atomisation process, or impurities picked up during solidification. Such particles initiate fatigue; the failure of an aeroengine turbine disc can be catastrophic.

2.2 Thermal Barrier Coatings

Increased turbine efficiency and reduced thermal effect is the main reason why thermal barrier coatings (TBCs) find their application in gas turbines [18]. A TBC system is usually composed of an MCrAlY bond coat (M=Ni and Co) which as a result of diffusion processes becomes the oxidation resistant layer and a yttria stabilized zirconia (YSZ) which is the top coat [18]. The TBC is an insulator in the system, and between the TBC and the superalloy, the bond coat provides a strong bond. There are two types of bond coats. One is (NiCo)CrAlY and the other is PtAl [19].Rich in Al , the TGO above the bond coat grows as the Al atoms in the bond coat react with oxygen which diffuse through the zirconia, which is transparent to oxygen [20]. Hence, the difference between the thermal expansion coefficients of the bond coat and the TGO causes the TGO to experience significant residual compressive stresses and strains during the heating and cooling of the system to and from service conditions [21-27]. These stresses and strain can induce deformation and cracking in the four layers of the TBC system [28]. The stresses and strains depend on the system‘s thermal loading history. They may results in ratcheting phenomena, microbuckling or cracking within the TBC [29-31].Isothermal exposure has been observed to result in different failure mechanism from those induced under cyclic thermal exposure. In general failure under thermal cycling occurs for TGO thickness of 1-5um, while failure under isothermal exposure occurs for TGO thickness of 5-15um. However, the underlying microstructural changes associated with failure phenomena in TBC are complex and difficult to model fully using mechanism-based models [29-31]. Thermal barrier coatings have been applied by electron beam deposition

physical vapor deposition [32], plasma spray technique [32] and other processing techniques that may result in the formation of a thin film deposits.

By increasing the entry gas temperature, the gas turbine efficiency can be improve by an [33] electron beam physical vapor deposited thermal barrier coatings in the hot compartment of advanced gas turbines [34]. Generally, the top coat that has been applied by EB-PVD technique comprises of a 100-200um thick layer yttria stabilized zirconia which is columnar. The gap that separates these columns is between 0.1-1um and presents in-plane strain compliance to the coating. That is, the coating can stand thermal strain mismatch with the primary superalloys substrate [35, 36]. The use TBCs at high temperature results in the transfer of oxygen from the atmosphere through the top coat towards the bond coat [18]. This results in the formation of a thermally grown oxide layer on the bond coat [37]. Although this scale protects the substrate against further oxidation, the growth of TGO during thermal cycling can lead to the failure of the TBC [18].

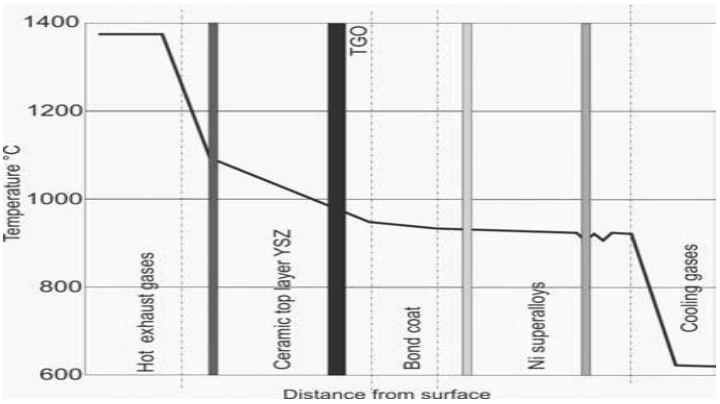

Figure 2. 3: *Distribution of temperature on surface of an element after having applied the TBC covering* [36-37]

2.2.1.0 Processing of Thermal Barrier Coatings

Like environmental barrier coatings(EBCs) thermal barrier coatings(TBCs) are processed by either plasma spraying or electron beam physical vapor deposition(EB-PVD) technique[32]. These give rise to layered microstructures with columnar 7.5-8.0 mole % Y_2O_3-ZrO_2 layers attached to PtAl or MCrAlY (M=Ni, Co) [38] bond coats and thermally grown oxide (TGO) layers that are formed by inward diffusion of oxygen and outward diffusion of Al [39]. One possible explanation of the presence of the TGO is the rapid nucleation of alpha- alumina, which has been shown by Tolpygo and Clarke[40] to form extensively over the surface of several TBCs. Tolpygo and Clarke have also shown that alpha aluminum nucleate more rapidly on grit blasted PtAl surface , to the exclusion of gamma or theta alumina.

2.2.1.1 Microstructure of Thermal Barrier Coatings

Microscopic analysis from Energy Dispersive Spectroscopy (EDS) and Scanning Electron Microscopy (SEM) have shown that chemical intermixing occurs with the TBC due to inter-diffusion of constituent elements from the work done by Yanar et al [41] The extent of the inter diffusion has been shown to depend on the exposure temperature. In the case of the isothermal oxidation, the growth of the alpha Alumina TGO layers is clearly apparent with increasing exposure duration at 1100^0C [41]. These have been shown to exhibit parabolic oxidation kinetics at 1100^0C [42]. However, at temperatures above 1100^0C, rapid linear oxidation kinetics has been reported, indicating the potential breakdown in the environmental protection that can be provided by conventional TBCs.

The use of heavy elements such as Hf have been explored to slow down the oxidation kinetics [40]. This has been shown to reduce the rate of TGO formation, compared to those in the conventional TBCs without heavy element doping.

Below is the cross sectional image of a thermal barrier coating as shown in figure 2.4.

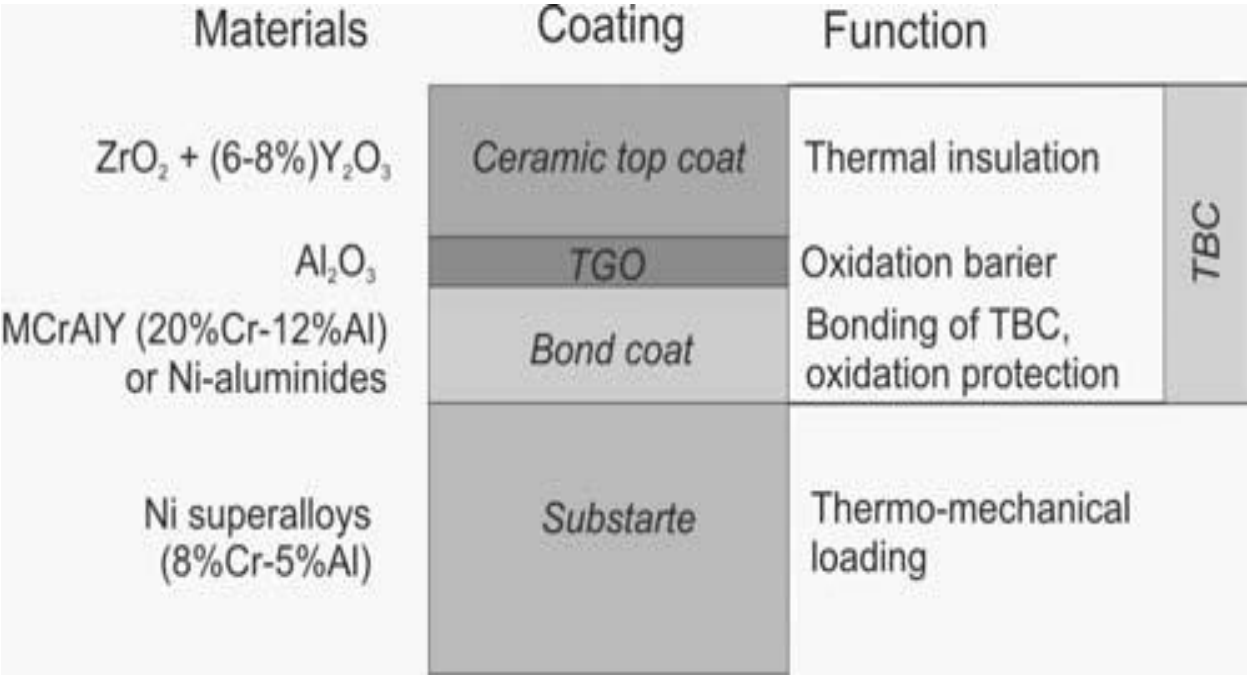

Figure 2. 4*: Scheme of coating construction of barrier layers and a role of individual sub-layers [43-44]*

2.2.1.2 Effects of Thermally Grown Oxide (TGO) layer on TBCs

The formation of TGO with increasing thermal exposure at temperatures between 1100^0C and 1200^0C has been shown to be associated with reductions in the interfacial fracture toughness (interface between the columnar Y_20_3 stabilized Zirconia and the TGO layer).

The use of indentation fracture toughness measurement suggests that the interfacial fracture toughness of EB-PVD deposited TBC structure decrease from ~3.8 to ~1 MPa $m^{0.5}$, after 60 hours of exposure at 1200^0C [42]. Also in the case of exposure at 1135^0C, the interfacial fracture toughness reduces to ~ 1MPa $m^{0.5}$ after 500hours, while the same level of 1MPa $m^{0.5}$ is reached after 100hours of exposure at 1100^0C. Such reductions in interfacial fracture toughness partly explain the susceptibility to spallation after prolonged exposure to isothermal oxidation at temperature between 1100^0C -1200^0C [42]. The buildup in strain energy as a result of coefficient of thermal expansion mismatch in the TBC system induces small cracks. These cracks grown and coalesce into larger cracks that are sufficient to form edge or center cracks that lead ultimately to coating delamination/spallation at the oxide/bond coat interface or oxide metal interface [24, 45].

2.3 Gamma-Based Titanium Aluminides

As the aircraft industry grows and the price of fuel increases, the overall weight of an aircraft becomes instrumental. As to whether a company makes profit or surrender to its competitors will depend on the company's ability to do research. Over the last 40 years, [46] a lot of research has gone into developing an alloy or an intermetallic compound that will address the issue of thrust and efficiency in both land based engines and aero engines. Gamma titanium aluminide has been a material of choice not only because of its weight [47] but also attractive mechanical properties and its higher melting temperature.

Gamma titanium aluminides (γ-TiAl) over the last few decades have been recognized to be suitable for aerospace applications due to their low density [48] and high strength at

elevated temperatures. On the other hand gamma titanium aluminides is an ordered intermetallic compound, though it is brittle at low temperature [46]. It is characterized by unique mechanical properties due to their long-range ordered crystal structure [49].This because of immobile dislocation, hence limiting the intermetallic application [49]. Since tailoring the microstructure of materials have significant effect on its properties, it is not impossible to design the intermetallic for a particular application. For example, employing metallurgical processing such a heat treatment can enhance microstructural properties. However, Electron Beam Melting (EBM) [49] in recent times been proven as a processing method to produce complex, near net shape γ-TiAl parts with short lead times. Figure 2.5 below shows the phase diagram for the intermetallic compound. The phase diagram of TiAl contains many different intermetallic compounds, such as Ti_3Al, TiAl, $TiAl_2$ and $TiAl_3$.

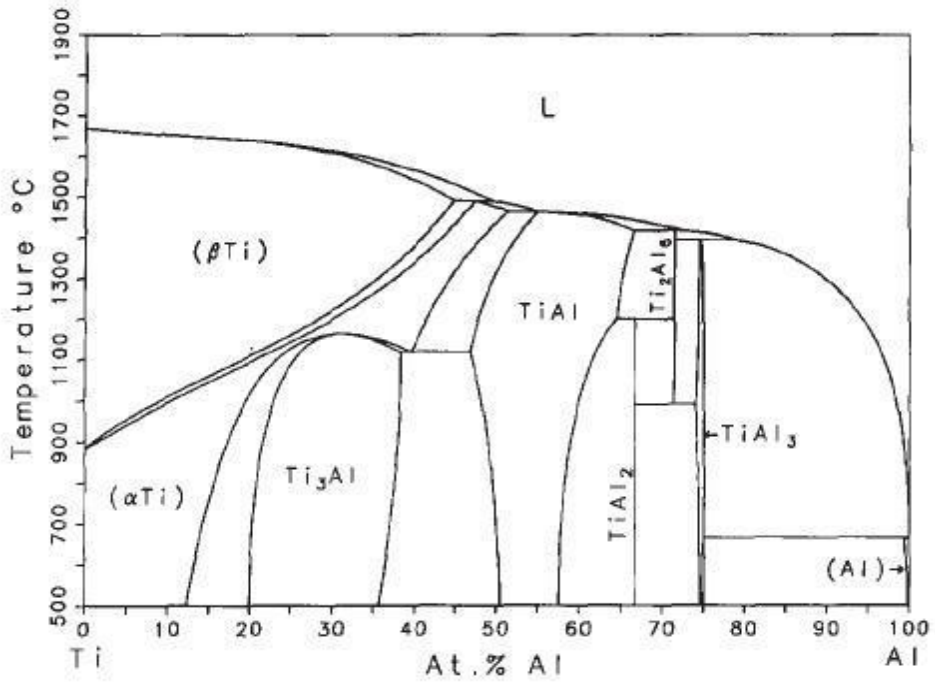

Figure 2. 5: ***Showing the phase diagram of titanium and aluminum adapted from ref [50]***

From the diagram above titanium alloys are those with aluminum atomic percent of approximately 8.5. In these types of alloys the possible phases formed are the alpha and betas. Alloys such as Ti-6Al-4V have these structures. The alloying elements have significant roles to play in the alloy. Aluminum stabilizes the alpha phase thereby increasing the c to a ratio and gives the alloy some form of ductility[49]. Vanadium on the other hand stabilizes the beta phase. In this case when the alloy is used in service some desired mechanical properties which would otherwise exist at high temperature is being maintained at room temperature.

Inter-metallics are formed as the composition of aluminum increases above 8 At. %. This intermetallic compounds are useful in structural applications and gamma titanium aluminide is an example [8]. This is because the two-phase structure between $\alpha_2(Ti_3Al)$ and γ(TiAl) results in improved mechanical properties. The microstructure and mechanical properties of TiAl alloys are strongly influenced by both the chemical composition and the heat-treatment procedures employed. Like titanium alloys, their intermetallics is also alloyed with elements such as Nb, Mo, Cr, V [51], B, or Si to improve its mechanical properties[52]. The additions of alloying elements such as Nb, Mn and Ta have been shown to have a greater influence on the transformation [53, 54]. This is because they increase the effective range of cooling rates and promote massive-γ formation [54].

Generally, chemistry and microstructure control the ductility and strength of gamma alloys. Around Al composition of 51 atomic percent [54], the Ti(43-55Al) exhibit its lowest strength. The elongation at room temperature differs with the aluminum content, it

displays a maximum and centered along the two phase composition (Ti-48Al). The volume ratio (5-15%) of $\propto_2$/y is the best ductility that have been postulated in Ti-48Al [55]. Above this, the brittle phase decreases the effect of ductilizing of refined microstructure. V, Cr or Mn additions in small amount in the dual phase composition (Ti-48Al) improves the ductility of the two phase gamma alloy [54]. Microstructural differences have direct influence on the room temperature tensile ductility and this ranges 0.5-4% plastic elongation [54, 55].

2.3.1.0 PROCESSING AND MICROSTRUCTURE CONTROL

Processing

A variety of processing methods are used to process gamma alloys. These methods are ingot metallurgy (IM), casting and powder metallurgy [54]. Plasma melting [39], induction skull melting and [51] vacuum arc melting are employed in melting gamma alloys. Investment casting has been used to produce near net shape products and component such as automobile exhaust valve [56], compressor or turbine blade and turbochargers. Porosity is normally removed by HIPing after lamellar cast ingot microstructures are formed [56]. HIPing can be costly especially in cases such as automobile engine valves. As a result, directional solidification is gaining more recognition since it produce similar mechanical properties [56]. Isothermal forging/extrusion or hot die forging are used in ingot metallurgy process on cast ingot which generally results in a non-uniform structure [56].

Below the alpha transus, hot working results in the recrystallization of fine grained microstructure in a (101) texture [57]. A cube-like texture component with the c-axis aligned to the transverse direction is normally shown during a hot packed rolled ingot which results in a plastic flow anisotropy. The peak stress and recrystallization strongly depends on the texture developed [56].

2.3.1.1 Ti-48Al-2Cr-2Nb

Gamma TiAl is a class of intermetallic compound that have found its applications in several industrial application. These industries include aerospace and car manufacturing

industries [49]. Research has shown that the processing of the intermetallic is expensive [49]. This is because in some cases the starting material is metallic powders. Also, the brittle nature of some gamma TiAl intermetallic makes it difficult to form shapes [49]. The Ti-48Al-2Cr-2Nb composition was first discovered by general electric corporate research center in the late 1980's [48]. The Ti-48Al-2Cr-2Nb has better mechanical properties such as improved toughness and ductility at lower temperatures as well as good creep properties [58]. With this composition the Ti-48Al-2Cr-2Nb is easier to process at ambient temperature [59].

Alloying element such as chromium increases the ductility and improves upon the workability of the material [60]. Increasing the chromium concentration in the intermetallic has been observed to improve the oxidation resistance [61]. Niobium has also been known to increase the oxidation and creep resistance of the intermetallic. The aforementioned function is possible because Nb slow down diffusion in TiAl alloys [60].

At 800^0C, the oxidation resistance the intermetallic is considered sufficient. Above 800^0C, there is decreased in oxidation resistance as a result of the formation of a non-protective oxide (TiO_2) rather than Al_2O_3. It has been observed below 800^0C that the less protective TiO_2 is formed. Al_2O_3 is however formed below 800^0C but at a higher density. Four different oxides are formed below 800^0C [49].

The figure below shows the various different types of oxides layers [49].

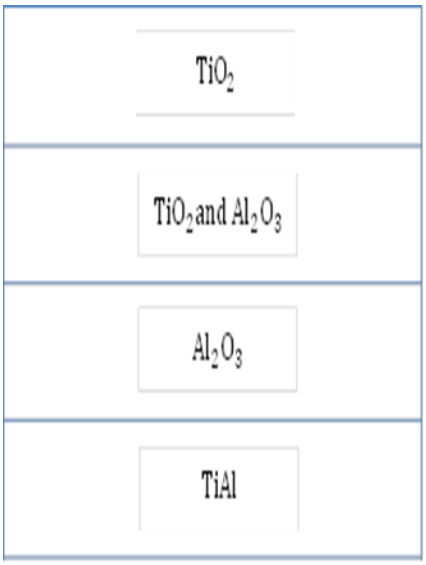

Figure 2. 6: ***Different oxide layers formed below 800^{0}C.***

2.3.1.2 Applications where TiAl have been used:

The divergent flap has been shown to be fabricated from wrought TiAl sheet [62]. This form of fabrication provide cost and weight saving. A hybrid of cast TiAl substructure and wrought TiAl may also be used to make the nozzle side wall. Various configuration of sheet have been fabricated and these shapes have reached the implementation stage [62]. Example of which are sheet configurations hot die produced at elevated temperatures joined by diffusion bonding and brazing [62]. Pratt and whitney have employed this method for producing aircraft corrugations as deep as 8.25cm from a 0.10cm starting sheet thickness [63]. Truss cores have been manufactured from TiAl sheet by BF Goodrich Aerospace [64] which is separately formed corrugation with face sheets of the same material. Other potential aerospace application for gamma TiAl alloys includes low pressure turbine blades and some structural applications [49].

References:

[1] Suzuki, Akane and Tresca M. Pollock. “High Temperature strength and deformation of y/y’ two phase Co-Al-W based alloys.” Acta Materialia 56.6(2008): 1288-1297.

[2] http://www.isis.stfc.ac.uk/science/materials-engineering

[3] Viswanathan, R, and W. Bakker. “ Materials for ultrasupercritical coal power plants-Turbine materials: Part II. Journal of materials engineering and performance, 10.1(2001): 96-101.

[4] Johnson, J.B., et al. “The mechanical properties of surface scales on nickel based superalloys-II. Contaminant corrosion.” Corrosion Science 18.6(1978):543-553.

[5] Tan, L., et al. “Corrosion behavior of Ni-base alloys for advanced high temperature water- cooled nuclear plants.” Corrosion Science 50.11(2008): 3056-3062

[6] Ezugwu, E.O.,Z.M.Wang, and A.R. Machado. “The machinability of nickel based alloys: a review.” Journal of Materials Processing Technology 86.1(1998): 1-16.

[7] http://www.ratnashreesteel.com/alloysteel.html

[8] Soboyejo, W. "Introduction to Advanced Materials", Materials Engineering, 2006.

[9] http://www.insg.org/%5cdocs%5cinsg_insight_20_nickel_alloys_2013.pdf

[10] W. Betteridge, S.W.S Shaw, Mater. Sci. Tech. 3 (1987) 682

[11] C.T. Sims, N.S. Stoloff, W.C. Hagel, Superalloys II: High-Temperature Materials for Aerospace and Industrial Power, New York: John Wiley and Sons (1987)

[12] K.A. Green, T.M. Pollock, H. Harada, Superalloy 2004: Proceedings of the Tenth International Symposium on the Superalloys, TMS (2004)

[13] D.D. Krueger, R.D. Kissinger, R.D. Menzies, C.S. Wukusick, U.S. Patent 4,957,567

[14] S.T. Wlodek, M. Kelly, D.A. Alden, in: R.D. Kissinger, D.J. Deye, D.L. Anton, A.D. Cetel M.V. Nathal, T.M. Pollock, D.A. Woodford (Eds.), Superalloys, Warrendale (1996) 129

[15] Tresa M. Pollock and Sammy Tin, Nickel-Based Superalloys for Advanced Turbine Engines: Chemistry, Microstructure, and Properties, Journal of Propulsion and Power Vol. 22, No. 2, March–April 2006.

[16] Pollock, T. M., and Murphy, W. H., "The Breakdown of Solidification in High Refractory Nickel-Base Superalloys," *Metallurgical and Materials Transactions*, Vol. 27A, No. 4, 1996, pp. 1081–1094.

[17] Walston,W. S., Cetel, A., MacKay, R., O'Hara, K., Duhl, D., and Dreshfield, R., "Joint Development of a Fourth Generation Single Crystal Superalloy," *Superalloys 2004*, TMS, Warrendale, PA, 2004, pp. 15–24.

[18] Saremi, M.. "Microstructural analysis of YSZ and YSZ/Al_2O_3 plasma sprayed thermal barrier coatings after high temperature oxidation", Surface & Coatings Technology, 2008/04/15

[19] S.Bose and J.DeMasi-Marcin "Thermal barrier coating experience in gas turbine engines at Pratt and Whitney" J. Thermal Spray Tech.6:99-104, 1997.

[20] Wang, Y., "Commercial thermal barrier coatings with a double-layer bond coat on turbine vanes and the process repeatability", Surface & Coatings Technology, 20090530

[21] D.M. Lipkin and D.R. Clarke,Oxid. Metals, 45,267-280(1996).

[22] V.K. Tolpygo and D.R. Clarke, Oxid. Metals, 49, 187-211(1998).

[23] C. Mennike, E. Schumann, C. Ulrich and M. Ruehle, Mater. Sci. Forum, 389,251-254,(1997)

[24] V. Sergo and D.R. Clarke, J. Amer. Ceram. Soc.81, 3237-3242(1998)

[25] V.K. Tolpygo and D.R. Clarke, Acta mater, 46, 5153-5166(1998)

[26] R.J. Christensen, V.K. Tolpygo and D.R. Clarke, Acta mater.,45, 1761-1766(1997).

[27] C.Sarioglu, J.R. Blachere, F.S. Petit and G.H. Meier, in Microscopy of oxidation 3, S.B. Newcomb and J.A. Little, eds., The Institute for Materials, London, (1997), p.41.

[28] Portinha, A.. "Residual stresses and elastic modulus of thermal barrier coatings graded in porosity", Surface & Coatings Technology, 2004/11/12

[29] M.Y. He, A.G. Evans and J.W. Hutchinson.Phys. Status Solidi A, 166(1):19 1999

[30] A.G. Evans, J.W. Hutchinson and M.Y. He. Acta mater. ,47(5) :1513, 1999.

[31] J.W. Hutchinson, M.Y. He. And A.G. Evans. J. Mech. Phys. Solids 48:709,2000.

[32] W.O. Soboyejo,P.Mensah, R. Diwan, J. Crowe and S. Akwaboa, High Temperature Oxidation Interfacial Growth Kinetics in YSZ Thermal barrier Coatings with Bond Coatings of NiCoCrAlY with 0.25% Hf, Materials Science and Engineering A, Vol. 528, page 2223-2230, 2011

[33] Deng, H.X.. "Effect of heat treatment at 900^oC on microstructural and mechanical properties of thermal barrier coatings", Surface & Coatings Technology, 2011/03/15

[34] Carton, Marc, Ennis, Philip James, Lecomte-Beckers, Jacqueline and Schubert, Florian. "Materials for Advanced Power Engineering 2006", Forschungszentrum Jülich, Zentralbibliothek, Verlag, 2007.

[35] Gell, M., "Bond strength, bond stress and spallation mechanisms of thermal barrier coatings", Surface & Coatings Technology, 1999/01/01

[36] G. Moskal, Thermal barrier coatings: characteristics of microstructure and properties, generation and directions of development of bond, Journal of Achievements in Materials and Manufacturing Engineering 37/2 (2009) 323-331.

[37] W. R. Chen. "The Oxidation Behavior of TBC with Cold Spray CoNiCrAlY Bond Coat", Journal of Thermal Spray Technology, 11/17/2010

[38] T. Chang, C. Mercer, M. Walter and W.O. Soboyejo. “An investigation of the Effects of Isothermal Exposure on Microstructural Evolution and Oxidation in a Thermal Barrier Coating”, Key Engineering Materials vol.197(2001) pp.185-198.

[39] Zhao, X.. "Spinel formation in thermal barrier systems with a Pt-enriched γ-Ni + γ′-Ni3Al bond coat", Surface & Coatings Technology, 2008/03/25.

[40] D.R. Mumm and A.G Evans, Acta Materialia, Vol .48., pp.1815-1827, 2000.

[41] N.M. Yanar, M.J. Stiger, M. Maris – Sida, F. S. Pettit and G.H. Meier, The effects of high temperature exposure on the Durability of Thermal Barrier Coatings, Key Engineering Materials Vol. 197, pp. 145-164, 2001. Trans Tech Publishers, Switzerland.

[42] R.A Handoko, J. L. Beuth, G.H. Meier, F.S. Pettit and M.J. Stiger, Mechanisms for Interfacial Toughness Loss in Thermal Barrier Coating System, Key Engineering Materials, Vol. 197, pp. 165-184, 2001. Trans. Tech. Publishers, Switzerland.

[43] U. Schultz, et al., Some recent trends in research and technology of advanced thermal barrier coatings, Aerospace Science and Technology 7(2003) 73-80.

[44] G. Moskal, Thermal barrier coatings: characteristics of microstructure and properties, generation and directions of development of bond, Journal of Achievements in Materials and Manufacturing Engineering 37/2 (2009) 323-331.

[45] S.R. Choi, J.W. Hutchinson and A.G. Evans, Mech. Mater., 31, 431-447(1999).

[46] ASM International. ASM Handbook Online - Ordered Intermetallics. C Liu and J.O Stiegler. Ordered Intermetallics. 2002.

[47] Ashby, Michael F. *Materials Selection in Mechanical Design.* Amsterdam : Elsevier Butterworth-Heinemann, 2005.

[48] Bartolotta, P, et al. The Use of Cast Ti-48Al-2Cr-2Nb in Jet Engines. *Journal of Material (JOM).* 1997, pp. 48-50, 76.

[49] Sanna Fager Franzén, “γ-Titanium Aluminide Manufactured by Electron Beam Melting”, thesis, 2010.

[50] Cupid, M Damian. *Thermodynamic Assessment of the Ti-Al-Nb, Ti-Al-Cr and Ti-Al-Mo Systems*. Gainesville : University of Florida, 2009.

[51] Carton, Marc, Ennis, Philip James, Lecomte-Beckers, Jacqueline and Schubert, Florian. "Materials for Advanced Power Engineering 2006", Forschungszentrum Jülich, Zentralbibliothek, Verlag, 2007

[52] Sreenivasulu G, Singh AK, Mukhopadhyay NK and Sastry GVS, “Effect of alloying and aging on morphological changes from lamellar to equiaxed microstructure of α2+ γ titanium aluminides”, *Metallurgical and Materials Transactions A*. 2001; 36(10):2603-2607.

[53] Hu D, Huang AJ and Wu X. On the massive phase transformation regime in TiAl alloys: The alloying effect on massive/lamellar competition. *Intermetallics*. 2007; 15(3):327-332.

[54] *Y-W.* Kim, *High Temperature Ordered Intermetallic Alloys IV*(Pittsburgh, PA: MRS, 199), pp. 777-793

[55] *Y-W. Kim. J0M,* 41 (7) (1989), pp. 24-30.

[56] Young-Won Kim. "Ordered intermetallic alloys, part III: Gamma titanium aluminides", JOM, 07/1994

[57] M. Nobuki and T. Tsujimoto., *JIMIS-6 Proc., on Intermetallic Compounds* (Sendai, Japan: JIM, 1991), *pp.* 451-456.

[58] Austin, C M, et al**.** Aircraft Engine Applications for Gamma Titanium Aluminide. M V Nathal, et al. *Structural Intermetallics 1997.* s.l. : TMS, 1997, pp. 413-425.

[59] Recina, Viktor. *Mechanical Properties of Gamma Titanium Aluminides.* Göteborg : Chalmers University of Technology, 2000.

[60] Westbrock, Jack Hall and Fleischer, Robert Louis**.** *Intermetallic Compounds Principles and Practice - Volume 2 Practice.* West Sussex : John Wiley & Sons Ltd, 1995.

[61] Huang, Shyh-Chin**.** Alloying Conciderations in Gamma Based Alloys. R Darolia, et al. *Structural Intermetallics.* Champion, Pennsylvania : The Minerals, Metals Minerals Society, 1993, pp. 299-307

[62] E.A. Loria., "Gamma titanium aluminides as prospective structural materials," Intermetallics (2000) 1339 -1345.

[63] Das G., Forming and joining of sheet gamma titanium aluminide. Presented at Aeromat 99, Dayton, 23 June 1999.

[64] Bartolotta P. NASA aerospace materials processing technology transfer to industry. GRC news release 99-79, 8 October 1999.

Chapter Three

3.1 Modeling

3.1.1.0 Fabrication of the thermal barrier coating

One of more common fabrication techniques is plasma spray processing where ceramic powder is melted and sprayed onto a substrate. This process renders a unique microstructure consisting of voids and defects within a porous coating microstructure. Moreover, many coating material properties differ from those of the corresponding bulk materials. For example, the elastic modulus of zirconia-based coatings is only about one fourth of that of bulk zirconia (Herman and Shankar, 1987; McPherson,1989; Bengtsson and Johannesson, 1995).

3.1.1.1 Composition and assumption for the TBC system

The TBC system is composed of an Inconel 617 substrate, a MCrAlY bond-coat and an air plasma-sprayed ceramic top-coat (Yttria Partially Stabilized Zirconia, ZrO_2–7.5 wt.% Y_2O_3) that gives rise to an Al_2O_3 thermally grown oxide.

However, the fabrication (blasting step) results in interfacial roughness in the TBC/BC and introduces compressive stress. Buckling occurs after the deposition process with completely different wavelength and amplitude in the ceramic/metal interface. Reproducing a real interface shape is very significant in the model since the outcome would be close to some experiments conducted. Hence, the calculation time requested will be long. For these reasons, the geometries associated to the numerical simulations

were ideally considered as a semielliptical shape and reduced to a region covering only a half period by using symmetry on the left side of the model and periodicity boundary condition on the right side of the model. The semi ellipse interface is of a wavelength of 20um and amplitude (A) ranging between 200um and 300um.

3.1.1.2 Material Model

The coating system considered is a ceramic-metal-metal configuration. ZrO_2- 7.5 wt Y_2O_3 is the ceramic surface coating chosen. At high temperatures (> 1100^0C) YSZ is known to creep, therefore it has been assumed to remain linearly elastic for the temperature range considered in this case. YSZ is modeled as an isotropic material. The YSZ and NiCoCrAlY chosen for the surface and bond coats are usually softer that the bulk material. Most thermally sprayed TBC contains 10 to 20% volume fraction of voids and cracks. The cracks cause the coating to reduce the thermal strains built up in the TGO. The bond coat and the substrate can deform plastically because they are made of metal based materials. The yielding of the bond coat and substrate affects the remnant stresses and fracture parameters of the TBCs. This is very significant in understanding the mechanical characteristics of the TBC under thermal loads at high temperatures. In this model, the bond coat is assumed to be air plasma sprayed NiCoCrAlY while the substrate is modeled as bulk Ni single crystal. The analysis depicts the YSZ coat and NiCoCrAlY bond coat as two distinct layers. However, it should be noted that the transfer of oxygen through YSZ causes the oxidation of some metal elements especially aluminum in the bond coat results in the formation of the TGO (Lee et al 1989). From the mechanical perspective, a very thin layer should not affect the structural response of the TBC. However, the effect can be detrimental depending on the nature of the oxide film.

3.1.1.3 Material Data

Material data used in the simulation are shown in Table 3.1. The material data provide in the table below are given at room temperature. Throughout this work the thermally grown oxide layer (TGO) is assumed to be alpha Al_2O_3. The materials in TBCs are assumed to be homogeneous and isotropic.

Table 3. 1 **Material Properties of the TBC coating system at room temperature**

Material Property [2]	Top Coat	Bond Coat [2]	Thermally Grown Oxide layer	Substrate 1(Inco HX) [2]	Substrate 2 (γ-TiAl)
Modulus(GPa)	48 [7]	152[9]	481 [1]	207	170
Density(Kg/m^3)	6208 [2]	7320	1281.5	8880	3900
Coefficient of Thermal Expansion(m/m)	9.11E-06 [2]	1.4E-05	5.07E-06 [9]	1.27E-05	12.2E-06
Poisson Ratio	0.2625 [2]	0.3	0.23 [7]	0.312	0.21
Thermal Conductivity (W/m-K)	2.7 [2]	4.3	30	90.5	28
Specific Heat(J/Kg)	517 [2]	501	718	416	419

3.1.1.4 TBC Design and Architecture

Temperature Effects (Oxidation Model)

An axisymmetric deformable part was selected to reduce the complexity of data and time. It was also used create the various layers (top coat, thermally grown oxide layer, bond coat and the nickel/ Ti-48Al-2Cr-2Nb substrate as the case may be) of the TBC system. These parts were created separately and later assembled. The thickness of the top coat, TGO, bond coat and the substrate were 330um, 0.3um, 234.7um and 3125um respectively. The thickness of the various layers mention was measured from the work done by Soboyejo et al using imageJ software. The material properties as shown in table 3.1 were assigned to the various layers. Vertical cracks (a=2um-100um) were introduced into the top coat. This is because these cracks are intentionally introduced in the deposition of the top coat to prevent the build-up of strain in the thermally grown oxide layer (TGO). The system was then meshed. The boundary conditions of the temperature were fixed, that at 0^0C (initial) and no displacement in the x-axis. The temperature load was applied from the top coat; that is the system was oxidized at a various temperatures (700^0C, 800^0C, 900^0C, 1000^0C and 1100^0C) and at different times (25, 50, 75, 100hrs).

$$\Delta\boldsymbol{\sigma} = \bar{\boldsymbol{E}} \propto (\boldsymbol{T_i} - \boldsymbol{T_0}) \qquad \textbf{(1)}$$

3.1.1.5 Steady State Heat transfer

Thermal gradient in the TBC

This study depicts a coupled steady state and thermal stress analysis. A slow heating /cooling process is assumed in the case of steady state. Uniform temperature is applied to the top surface of the YSZ coat. Within the top coat and bond coat there is a decrease in temperature with increasing depth until the interface between the bond coat and substrate is reached. The temperature field of the substrate is modeled to be constant since the substrate has a much higher thermal conductivity than the top coat. The insulation effect of the TBC results in the drop in temperature. Microstructure and transient boundary temperature makes it difficult to obtain the actual temperature distribution in high temperature conditions. The difference between surface and substrate temperature have been assumed to vary linearly with the imposed temperature at the surface.

3.1.1.6 Geometry and Model Description

The model geometry is that of a solid cylinder which is thought to be infinitely extended in its axial direction. It consists of a nickel superalloy and gamma titanium substrate with a radius of 6000 um and 3000um respectively as shown in fig. 3.1 and 3.2. The average thickness of the top coat, thermal grown oxide layer, bond coat and the substrate are 330um,0.3um,234.7um and 3125um respectively. The geometry in fig 3.2 corresponds closely to that used by [7]. The finite element quad mesh consists of 692 nodes in the first case (fig 3.1) and 842 in the second case fig 3.2. The meshing is fairly fine in the region of the TGO/TC-interface. The model is constrained in the *y*-direction on the axis in order

to simulate a full cylinder with no inner hole. Vertical cracks were introduced to the top coat layer. The cracks had the same length in figure 3.1 whereas different crack lengths were considered in figure 3.2 at different TGO thicknesses. The model can be considered as a slice taken out of a sample that is very long and unconstrained in the *x*-direction.

MODEL 1 (GEOMETRY)

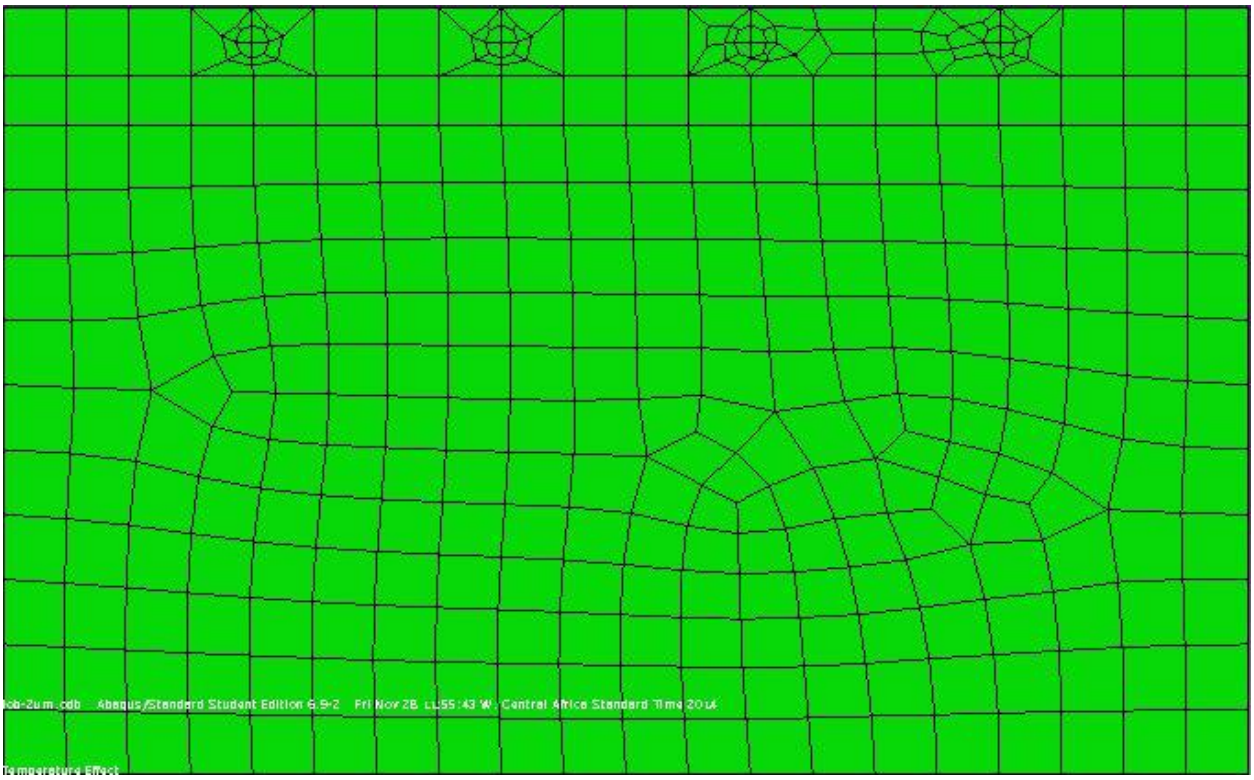

Figure 3. 1: ***shows the TBC model geometry with an initial TGO thickness of 0.3um***

MODEL 2(GEOMETRY)

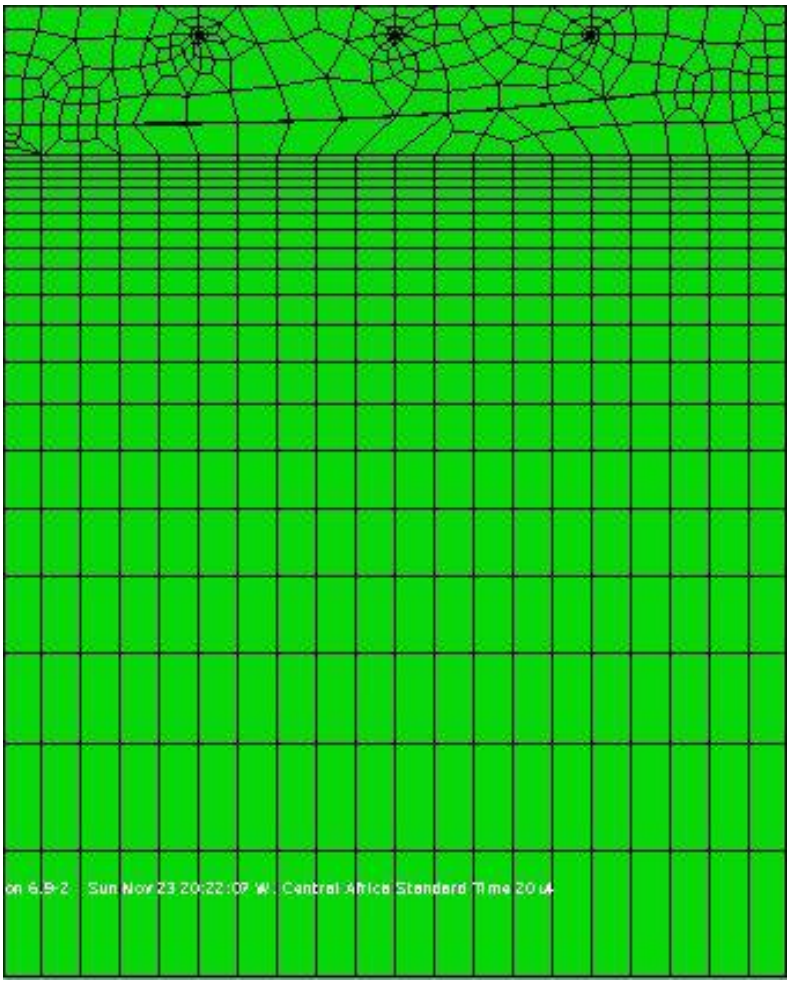

Figure 3. 2: ***shows the TBC model geometry with the buckling effect.***

3.1.1.7 Crack Model

Four Cracks were introduced to the top coat (YSZ layer) of the thermal barrier coating. The crack length was 10um for long cracks and 3-5um for short cracks in both model geometries as shown in figures 3.1 and 3.2 respectively. The seam option was used to create the cracks in ABAQUS 6.9 student version with contour integral. The model was subjected to isothermal heating to determine the effects of thermal stresses on crack growth. The vertical cracks are necessary because some deposition techniques such as the

Air Plasma Spraying (APS) results in cracks in the TBC system [10]. In this model the energy release rate and stress intensity factor was calculated at different temperatures since the isothermal heating results in thermal stresses. The governing equation of plane strain stress intensity factors are shown below.

$$K_I = \frac{\delta_I}{\delta}\sqrt{\frac{GE}{1-\vartheta^2}} \quad \text{..... (2)}$$

$$K_{II} = \frac{\delta_{II}}{\delta}\sqrt{\frac{GE}{1-\vartheta^2}} \quad \text{..... (3)}$$

δ- Magnitude of crack opening displacement E- Tensile Modulus G- Energy release rate

ϑ- Poisson ratio K- stress intensity factor

The subscript I and II represents mode I and mode II

Reference:

[1] www.engineeringtoolbox.com

[2] Seo et al. Finite Element Analysis of Residual Stress in NiCrAlY/yttria-stabilized Zirconia Coatings by Nanoscale Multi-layered Deposition. Key Engineering Materials Vols. 270-273 (2004) pp. 58-63.

[3] Antou G. Amélioration de revêtements barrière thermiques par un procédé de refusion laser in situ utilisant un laser à diodes. Ph.D. thesis, Strasbourg, June 2004.

[4] Pan D, Chen MW, Wright PK, Hemker KJ. Evolution of a diffusion aluminide bond-coat for thermal barrier coatings during thermal cycling. Acta Mater 2003; 51: 2205–17.

[5] Freborg AM, Ferguson BL, Brindley WJ, Petrus GJ. Mater Sci Eng A 1998;245:182.

[6] Frost HJ, Ashby MF. Deformation-Mechanism Maps. Oxford: Pergamon Press; 1982

[7] J. Rosler, M. Baker, K. Aufzug. A parametric study of the stress state of thermal barrier coatings Part I: creep relaxation. Acta Materialia 52 (2004) 4809–4817.

[8] HKS Inc. ABAQUS/Standard User's Manual, Version 6.9, USA; 1998.

[9] P. Bednarz, R. Herzog, O. Trunova, R.W. Steinbrech, H. Echsler, W.J. Quadakkers, F. Schubert, L. Singheiser, Proceedings of 29th International Conference on Advanced Ceramics and Composites, 20–25 January 2005, Cocoa Beach, USA, Advances in Ceramic Coatings and Ceramic-Metal Systems, Ceram. Eng. Sci. Proc. 26 (2005) 73.

[10] W.O. Soboyejo, P. Mensah, R. Diwan, J. Crowe and S. Akwaboa, High Temperature Oxidation Interfacial Growth Kinetics in YSZ Thermal barrier Coatings with Bond Coatings of NiCoCrAlY with 0.25% Hf, Materials Science and Engineering A, Vol. 528, page 2223-2230, 2011

Chapter Four

4.1 Results and Discussion

4.1.1 Energy Release Rate Studies

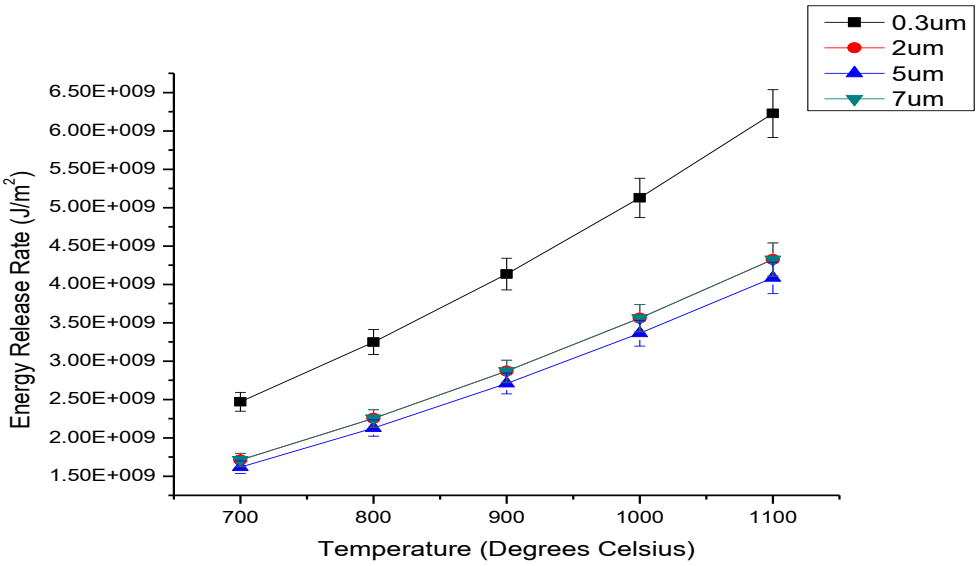

Figure 4. 1: *A graph of Energy release rate against temperature for TGO thickness of 0.3um, 2um, 5um and 7um without the buckling effect at steady state.*

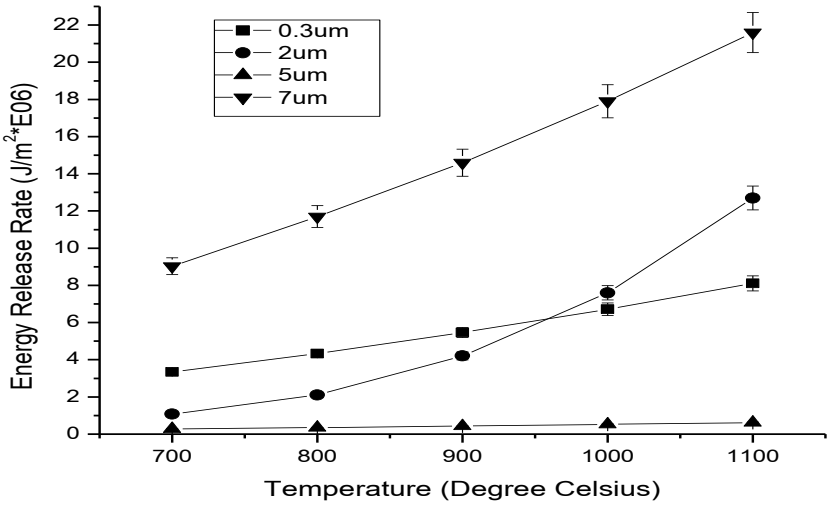

Figure 4. 2: ***A graph of Energy release rate against temperature for TGO thickness of 0.3um, 2um, 5um and 7um with buckling effect at steady state.***

$\Delta\boldsymbol{\sigma} = \overline{\boldsymbol{E}} \propto (\boldsymbol{T_i} - \boldsymbol{T_0})$ ..... (1)

$\boldsymbol{G_{ss}} = \frac{\boldsymbol{h}}{\boldsymbol{2E}}\left(\boldsymbol{E} \propto [\boldsymbol{T_o} - \boldsymbol{T_i}] - \boldsymbol{2T_{dep}}\right)^{\boldsymbol{2}}$ ..... (2)

G_{ss} – Steady State Energy Release Rate h- thickness of the TBC

E – Elastic Modulus $\propto$ –coefficient of thermal expansion

T_o – Temperature above 1000^{o}C T_i –Initial Temperature

T_{dep}- Applied Temperature

The energy release rate dependence on temperature is presented in figures 4.1 and 4.2 for various thermal grown oxide (TGO) thicknesses with non-buckling and buckling effects respectively. The energy release rate increases with increasing temperature in both cases, for fixed values of the TGO thickness. When a vertical crack emerges from an edge along the top coat (YSZ), the force and moment are released, giving rise to an energy release rate. The energy release rate for the system that has undergone buckling is 1000 times less than the non- buckled system. Figure 4.2 tends to show some abnormally because the crack length was varied the cracks in the TBC system may not have uniform crack length after buckling. The stresses within the top coat occur as a result of thermal mismatch stresses (equation 1). For a constant potential energy and crack length, the energy release rate depends on the thickness of the top coat, when the crack is initiated. The maximum value of the energy rates rate decreases as the TGO thickness increases for both cases.

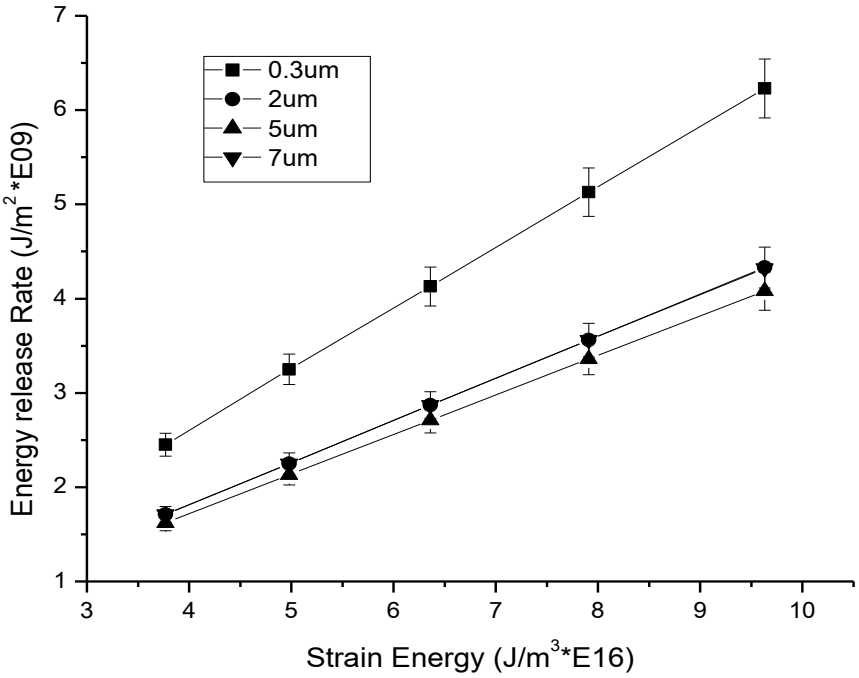

Figure 4. 3: ***Shows a plot of energy release rate against strain energy at different TGO thicknesses without buckling effect.***

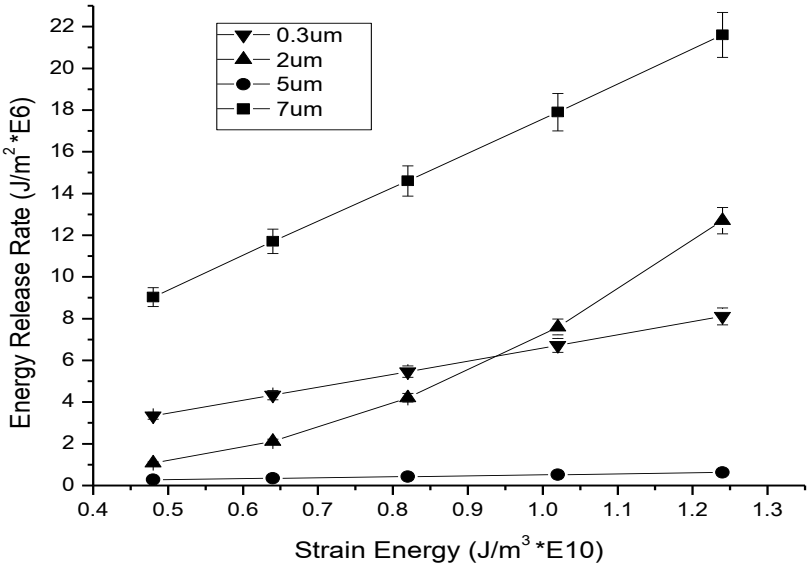

Figure 4. 4: ***Shows a plot of energy release rate against strain energy at different TGO thicknesses with buckling effect.***

The energy release rate dependence on the strain energy is presented in figures 4.3 and 4.4 respectively for both buckling and non-buckling effect. The energy release rate increases with increasing strain for the different TGO thicknesses. There is not much strain at the top/TGO interface for the initial TGO thickness of 0.3um and this corresponds to the highest value of the energy release rate in the TBC system in figure 4.3. The effects on buckling which can be linked to oxidation and mismatch in the coefficient of thermal expansion on the other hand tends to reduce the energy release rate by 10E3 as the strain increases.

4.1.2 Effects of Stress Intensity Factor and Strain Energy

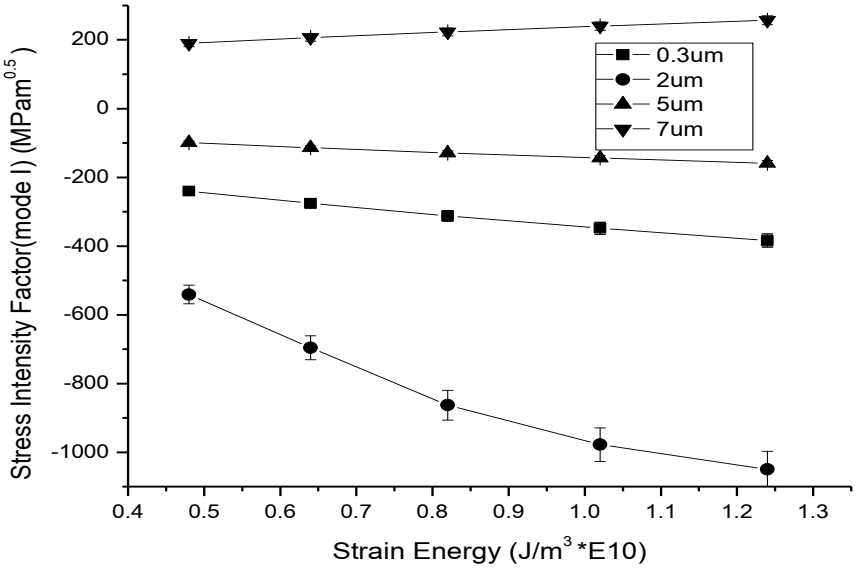

Figure 4. 5 ***Stress Intensity Factor (mode I) against Strain energy(buckling) for TGO thickness of 0.3um, 2um, 5um and***

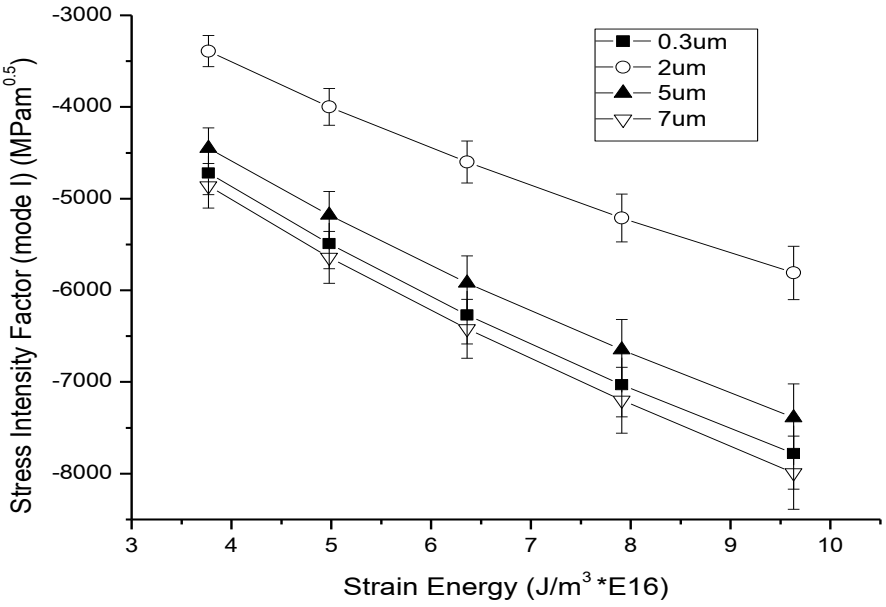

Figure 4. 6: ***Stress Intensity Factor (mode I) against Strain Energy (no buckling) for TGO thickness of 0.3um, 2um, 5um and 7um respectively*****.**

The mode I stress intensity factor decreases with increasing strain energy. As the oxide layer is increased to 5um, it however increases with increasing strain energy as the TGO thickness reaches a critical value of 7um in the buckling model as shown in figure 4.5. This is because of the changes in the remote or local stress state near the crack tip field. Tensile stresses are experience as the TGO layer reaches a critical value of 7um. Therefore the TBC coating system is likely to experience failure at a TGO thickness of 7um. The behavior of the graph can be attributed to the imperfections because they could either amplify or reduce stresses developed around them as the TGO grows. In instances relating to low thermal cycling, the stresses in the TBC are dominated by TGO growth.

Figure 4.6 the stress intensity factor increases which increasing strain energy which actually presents the exact opposite of what happens in figure 4.5. This is because in figure 4.6, the model has been assumed to have no effects of buckling. There is a

transition from negative stress intensity factor to positive values except that in figure 4.5 the stress intensity factor increases with increasing strain energy whereas in figure 4.6 the stress intensity factor decreases with increasing strain energy for a TGO thickness of 7um. The magnitude of the different modes of the stress intensity factor can be attributed to the crack opening displacement from the reference point in the model.

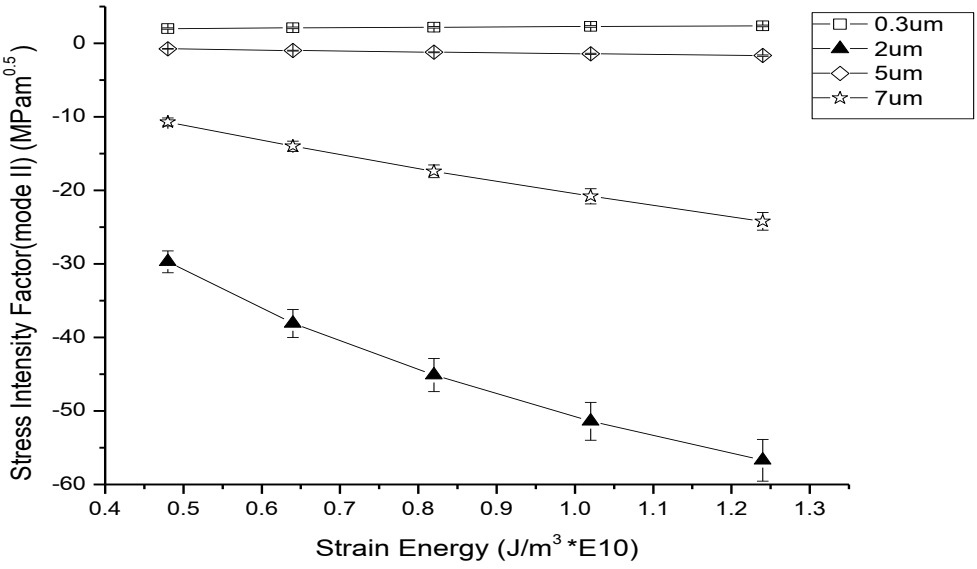

Figure 4. 7: ***Stress Intensity Factor (mode II) against Strain energy (buckling) for TGO thickness of 0.3um, 2um, 5um and 7um respectively.***

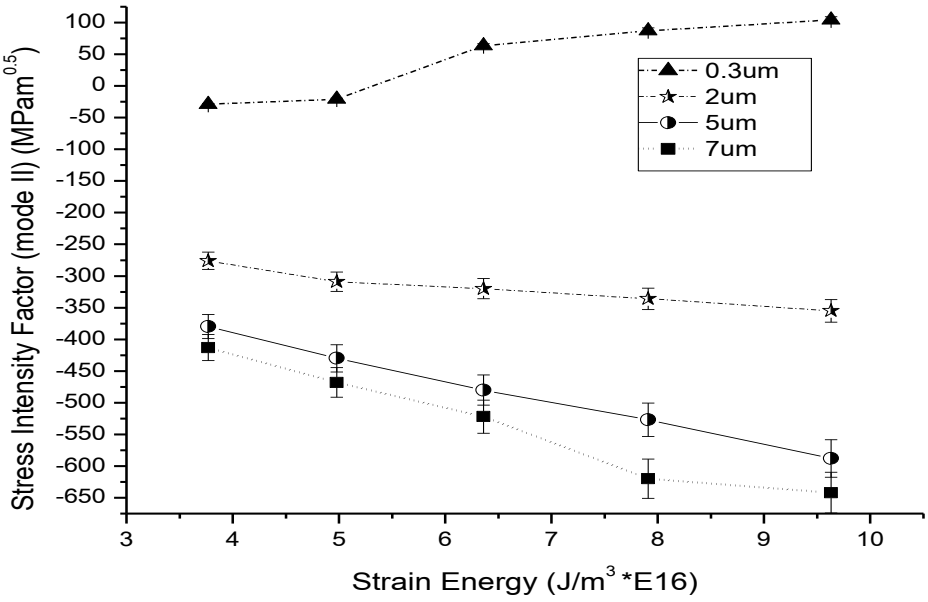

Figure 4. 8: ***Stress Intensity Factor (mode II) against Strain energy (no buckling) for TGO thickness of 0.3um, 2um, 5um and 7um respectively.***

The mode II or shear stress intensity factor is presented in figures 4.7 and 4.8 respectively. The stress intensity factor increases with increasing strain energy for the TGO thickness of 0.3um (figure 4.7). The values of the stress intensity factor then changes from positive to negative and decrease with increasing strain energy as the TGO thicknesses are increased to 7um.

Figure 4.8 depicts the opposite of what happens as the effects of buckling were not assumed. The value of the stress intensity factor decreases as the strain increases for the TGO thickness of 0.3um. It therefore increases as the strain energy increases as the TGO grows. The strain energy is increased by 10E6 as a result of relatively high in plane stiffness and limited strain tolerance. As the TGO thickness is increased the driving force for crack growth is increase since the critical fracture toughness is 3.5MPam$^{0.5}$ from reference 2 since maximum fracture toughness is 3312MPam$^{0.5}$. This however leads to

further cracking and finally failure. A discontinuous temperature field across the crack faces in a ceramic [3] coating i.e. YSZ can significantly increase the energy release rate. Essentially, the temperature jump over the crack enhances the thermal expansion difference in the regions above and below the crack and generates a large mode II or shear loading near the crack tip. Subsequently, the insulation across the crack faces may promote crack extension through increased crack driving force as shown in figures 4.7 and 4.8 for 0.3um.

4.1.3 Effects of Isothermal and Thermo mechanical Exposure on TBC

TBC sintering, oxide growth and loss of interfacial toughness due to thermo-mechanical and chemical damage are the principal factors that contribute to apparent loss in TBC robustness. During isothermal exposure, the TGO layer grows thicker as result of continued oxidation of the bond coat layer [2]. The elastic strain energy release rate increases as the TGO thickness increases. This suggests that the onset of crack growth is more likely to occur as the TGO thickness increases.

Furthermore, the increased waviness of the TGO (due to the buckling of the TGO) results in increasing strain energy that also increases the likelihood of cracking in the ceramic top coat. This again leads to the onset of crack growth in the ceramic top coat layer. Hence, the growth of the TGO and the buckling of the TGO are both likely to lead to the onset of cracking of the ceramic top coat.

However, as the duration of isothermal exposure increases, sintering of the yttria-partially stabilized zirconia layers also occurs. This leads to increased moduli [2]. The increase in

the TBC effective modulus is also associated with increasing compressive residual stresses at room-temperature [2]. This results in increased elastic strain energy that is available to propagate the crack.

4.1.4 Temperature Distribution

Figures 4.9 and 4.10 presents the respective temperature distribution in the gamma titanium aluminide and nickel alloy substrates, during exposure to a surface temperature of 1100^{o}C. The predicted temperatures are generally well below the recrystallization temperature of gamma based titanium aluminides (750K) and nickel based alloys (600K). Hence the microstructures are likely to remain stable. The significance of this model is to verify if there is going to be recrystallization. This is because recrystallization can cause a change in microstructure hence adversely affecting the mechanical properties of the substrate. It has been shown from literature that gamma titanium aluminides forms non protective layers such as TiO_2 above 800^{o}C which becomes dominant and results in failure by oxidation [1]. The recrystallization temperature of nickel substrate is $\sim$ 576K but from figure 4.4 the maximum value of temperature is 373K which means signifies that there will be no change in phase

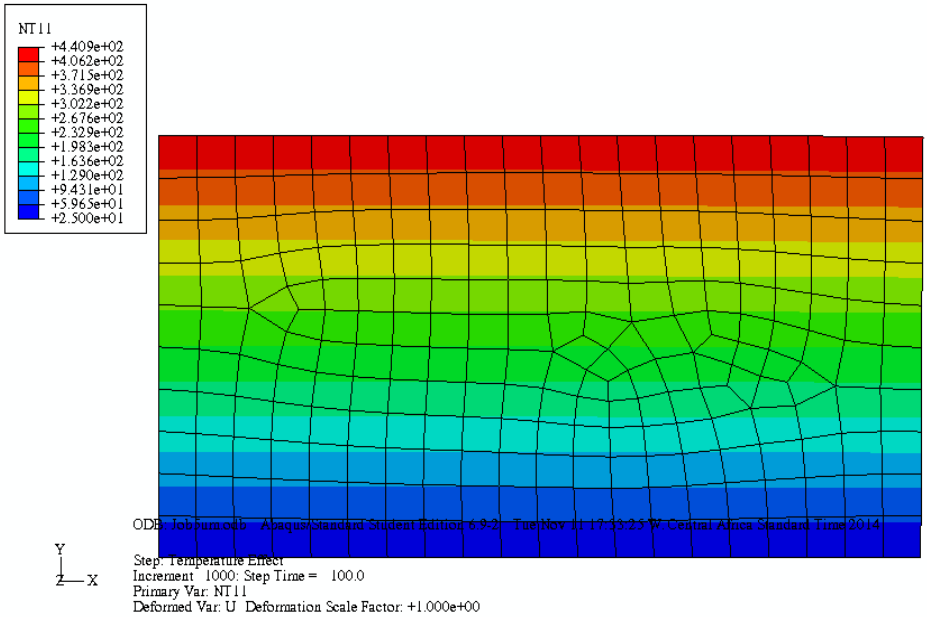

Figure 4. 9: *Temperature distribution across Titanium substrate (Ti-48Al-2Cr-2Nb) subjected to a temperature of 1100^{0}C at TGO thickness of 5um.*

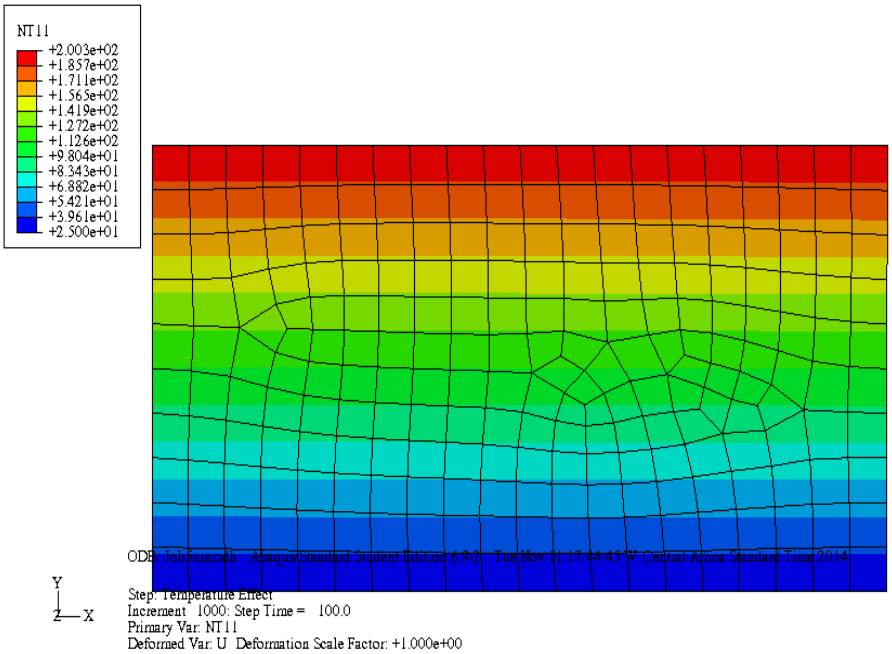

Figure 4. 10: *Temperature distribution across Nickel single crystal substrate (Inco HX) subjected to a temperature of 1100^{0}C at TGO thickness of 5um.*

4.1.5 Effect of Mode Mixity on Crack Driving Force

$$\boldsymbol{\varphi} = \tan^{-1}\frac{K_{II}}{K_I} \ldots\ldots\ldots\ldots\ldots\ldots\ldots\ldots\ldots\ldots\ldots\ldots\ldots\ldots\ldots\ldots \quad (4.1)$$

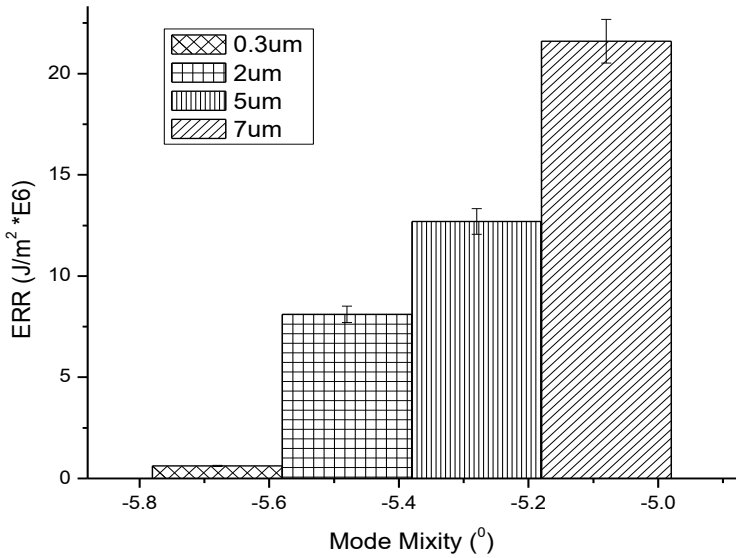

Figure 4. 11: ***A graph showing the energy release rate on the mode mixity (buckling) at different TGO thicknesses***

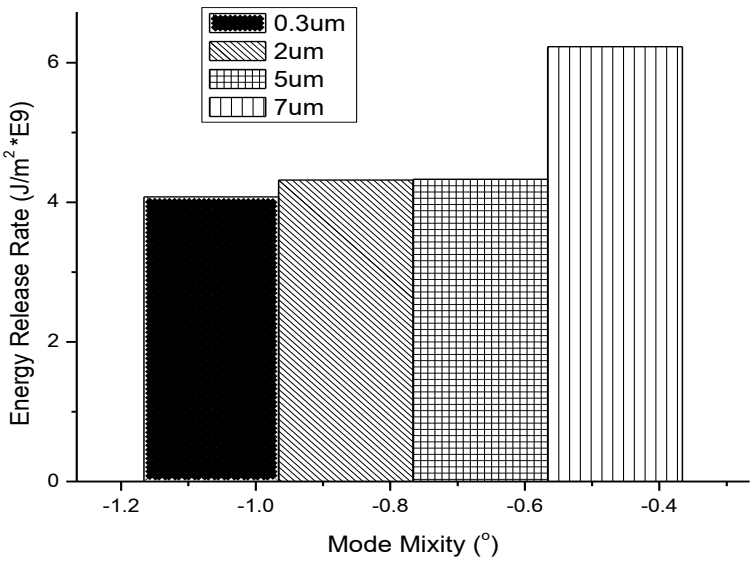

Figure 4. 12: ***A graph showing the energy release rate on the mode mixity (without buckling) at different TGO thicknesses***

When a crack is embedded in a layered medium, the mismatch of the adjoining material properties generates shear deformation near the crack tip. This causes the so-called 'mixed-mode' fracture even under symmetrical loading conditions. Since the fracture resistance given in terms of G is strongly dependent upon the ratio of the mode I and II stress intensity factors, it is essential to evaluate the mixed-mode K_I and K_{II} of a crack in the layered medium. In general, most cracks show higher critical energy release rate when K_{II} is relatively larger than K_I. In order to extract the stress intensity factors, a computational approach involving an interaction energy integral is used for cracks in linearly elastic materials. The interaction energy release rate is based on the principle of superposition, and it can be used to numerically separate $\boldsymbol{K_I}$ and $\boldsymbol{K_{II}}$**.** The domain integral formulation of the interaction energy release rate for the axisymmetric problems can be found in Nahta and Moran (1993) and Qian et al. (1997) [3]. Once $\boldsymbol{K_I}$ and $\boldsymbol{K_{II}}$ are extracted from the finite element solutions, the non-dimensional phase angle $\boldsymbol{\varphi}$ used to quantify the ratio of the shearing mode (mode II) to the opening mode (mode I).

The mode mixity increases with increasing TGO thicknesses as the energy release rate in both the buckling and unbuckled model (fig.4.11 and 4.12 respectively) increases. Though there are both negative and positive angles with respect to the mode mixity, the equation above confirms that the shear stress intensity factor is dominant. Therefore the driving force for crack growth in the TBC system is the net increase in mode II stress intensity factor relative to mode I as oxidation of the TGO progresses.

Reference:

[1] Sanna Fager Franzén, " γ-Titanium Aluminide Manufactured by Electron Beam Melting" ,thesis ,2010.

[2] R.A Handoko, J. L. Beuth, G.H. Meier, F.S. Pettit and M.J. Stiger, Mechanisms for Interfacial Toughness Loss in Thermal Barrier Coating System, Key Engineering Materials, Vol. 197, pp. 165-184, 2001. Trans. Tech. Publishers, Switzerland.

[3] G. Qian, T. Nakamura, C.C. Bemdt, "Effects of thermal gradient and residual stresses on thermal barrier coating fracture" Mechanics of Materials 27 (1998) 91 - 1 10.

Chapter Five

5.1 Implication

Using gamma based titanium aluminide in some section of the land based engine will help reduce the entire weight of the engine. Since the intermetallic has its density which is approximately half ($4.2g/cm^3$) that of nickel, the thrust of an aero-engine will be improved thereby reduce its fuel consumption should the intermetallic be used in that application. This has been shown in the temperature distribution in the computational modelling that has been carried out in chapter four.

5.2 Conclusion

The failure mechanisms of thermal barrier coatings have been examined through ABAQUS^{TM} FEM model of residual stress generation due to oxidation as a result of isothermal heating. The results show that oxidation has a direct effect on the stress intensity factor and energy release rate. Vertically cracked thermal barrier coating has been simulated in the study. The effects of stress that exist between the TC/TGO layer on the vertical cracked YSZ top coat have been discussed as being detrimental for a critical TGO growth of 7um. In reality the cracking in TBC systems is not confined only to the TGO/BC interface. It spreads into TGO and TBC and finally leads to coating spallation. From the temperature distribution in figures 4.9 and 4.10, we can conclude that TBC coated gamma titanium aluminide can be used in land based engines since the maximum temperature experience by the substrate is less than its maximum use temperature which is 538^0C. The driving force for crack growth in the thermal barrier coating system has

been identified as the net increase in thermal grown oxide layer (TGO). The TGO causes cracks to coalesce as a result of large scale buckling as the strain energy increases.

5.3 Recommendation

This progression of cracking is clearly a result of the combined action of creep, oxidation and thermal cycling. An accurate description of the entire process requires a model including these factors. However, failure of a TBC is very complex and is clearly not completely described by a simple model. Other factors, such as: sintering; phase changes in the oxide, bond coat and ceramic layer; ceramic layer cracking; and compositional changes are also thought to be important aspects that should be included for a complete description of the failure mechanisms.

5.4 Future Work

A key message of the present work is the sensitivity of the isothermal oxidation of the thermally grown oxide (TGO) layer and its influence on stress intensity factor and energy release rate. Definitely a creep aspect needs to be considered for future material improvement in order to successfully predict the failure of TBC for land based engines.